NASA CR-168001
Contract NAS7-918
Task Order RE-65, Amendment 399

Ion Accelerator Systems for High Power 30-cm Thruster Operation

Final Report

By
Dr. Graeme Aston
Electric Propulsion and Plasma Technology Group
Jet Propulsion Laboratory
California Institute of Technology
Pasadena, California

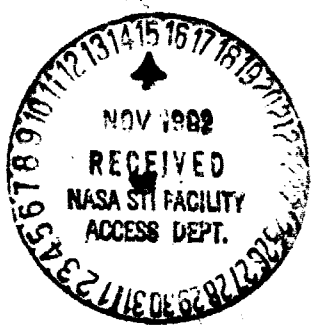

Prepared for
National Aeronautics and Space Administration
NASA Lewis Research Center
Vincent K. Rawlin, Program Manager

NASA CR-168001
Contract NAS7-918
Task Order RE-65, Amendment 399

Ion Accelerator Systems for High Power 30-cm Thruster Operation

Final Report

By
Dr. Graeme Aston
Electric Propulsion and Plasma
Technology Group
Jet Propulsion Laboratory
California Institute of Technology
Pasadena, California

Prepared for
National Aeronautics and Space Administration
NASA Lewis Research Center
Vincent K. Rawlin, Program Manager

Table of Contents

Page

Abstract 1

Introduction 2

Apparatus and Procedure 4

Two Grid Tests:

  Beam Deflection and Impingement 9

  Uniform Perveance Limit Grid Set 17

Three Grid Tests:

  Beam Deflection and Impingement 29

  Uniform Perveance Limited Operation 32

Summary 37

Acknowledgement 37

References 39

List of Illustrations

Figure		Page
1	Thruster Simulation Apparatus	5
2a	30-cm Thruster Plasma Density Profile	7
2b	Grid System Beam Current Fraction	7
3	Simulated SHAG Beamlet Deflection and Impingement Current Characteristics	10
4	Simulator Predictions of 30-cm Thruster Beamlet Deflection and Impingement	16
5a	Generalized SHAG Divergence Angle and Normalized Perveance Characteristics	18
5b	Predicted Limits of SHAG Accelerator System Operation	20
6	Experimental Verification of Uniform Perveance Grid Set Operating Limits	23
7	Comparison of Uniform Perveance Limited Grid Set and SHAG Grid Set Performance	25
8	Uniform Perveance Grid Set Thrust Loss	27

List of Illustrations Continued

Figure		Page
9	Uniform Perveance Grid Set Beamlet Deflection Capability	28
10	Simulated Three-Grid Beamlet Deflection and Impingement Current Characteristics	30
11	Simulator Predictions of a Three-Grid 30-cm Thruster	33
12	Uniform Perveance Three-Grid Set Beamlet Deflection Capability	34

Abstract

An investigation of two and three-grid accelerator systems for high power ion thruster operation has been performed. Two-grid translation tests show that over compensation of the 30-cm thruster SHAG grids leads to a premature impingement limit. By better matching the SHAG grid set spacing to the 30-cm thruster radial plasma density variation and by incorporating grid compensation only sufficient to maintain grid hole axial alignment, it is shown that beam current gains as large as 50% can be realized. Three-grid translation tests performed with a simulated 30-cm thruster discharge chamber show that substantial beamlet steering can be reliably affected by decelerator grid translation only, at net-to-total voltage ratios as low as 0.05.

Introduction

Ion thrusters are continually being pushed to high power levels of operation in an effort to produce the most thrust for a given thruster diameter, while still retaining acceptably long lifetimes with tolerable heat rejection requirements. Most recently, several workers have documented J-series 30-cm mercury ion thruster operation at power levels several times the baseline value for this thruster [1-3]. In general, relatively minor thruster modifications were implemented to provide operation at these much larger power levels. During the course of these high power ion thruster tests, excessive accelerator grid impingement currents were encountered as the thruster beam current level was increased beyond the nominal operating value of 2.0 ampere. To stay below this excessive accelerator system impingement limit it was necessary to continually increase the accelerator system electrode potentials as the thruster beam current was increased. Ideally, accelerator system grid potentials should be raised only when the extracted ion beam current would other wise exceed the accelerator system perveance limit. Exceeding the perveance limit, or over driving the accelerator system, simply means that repulsive ion space charge forces become dominant within the grid set accelerating gap. These forces result in ion beamlet blow up and direct accelerator grid ion interception. For the high power ion thruster tests, it was noted that the onset of excessive accelerator grid ion impingement occurred at beam current values less than expected from the design of the accelerator system with the specified average grid set gap and applied accelerating voltages. Although it was well known that the ion current density distribution across the 30-cm diameter thruster was quite non-uniform, it was not apparent where across

the diameter of this thruster the grid set was being over driven.

The first portion of this paper presents the results of a series of experiments designed to determine that region of a Small Hole Accelerator Grid (SHAG) 30-cm J-series thruster ion accelerator system where operation is limited by excessive accelerator grid ion interception. Based upon the results of these tests, an alternate two-grid accelerator system design philosophy for the J-series 30-cm thruster is evolved. Comparisons of simulated thruster performance at high beam powers with this alternate accelerator system design and conventional SHAG optics are presented.

The final sections of this paper are concerned with the correct application of a three-grid ion accelerator system to the J-series 30-cm thruster and the behavior of this type of thrust system at high beam power levels and very low beam energies (or specific impulse values). Knowledge of high power thruster operation at low specific impulse values is important because of the potential use of large thrust ion engines in the performance of low earth orbit to geosynchronous earth orbit payload transfer missions. Acceptably short trip times using electric propulsion for these missions are possible only if reliable high thrust 30-cm thruster operation can be achieved with values of specific impulse factors of several times lower than present baseline values.

Apparatus and Procedure

All the experimental results presented in this paper were obtained using a simulated J-series 30-cm thruster. This apparatus comprised an 8-cm diameter mildly divergent magnetic field filament cathode discharge chamber which operated on argon propellant. Coupled to this discharge chamber was an accelerator system assembly which could accomodate either a single hole two-grid or three-grid ion optical system. A resolving motor, driving a precision lead screw and thrust carriage, was coupled to the accelerator system assembly and allowed remote translation of the grid electrodes in the accelerator system geometry under test. The ion beam emerging from the accelerator system was scanned in a direction normal to the beam axis by a guarded Faraday ion probe located 33.4 cm from the accelerator system downstream surface. This probe was moved remotely through the ion beam by an A.C. gear motor and precision lead screw drive. The subsequent profile of beam ion current density as a function of probe position was recorded on an accompanying x-y recorder. Figure 1 illustrates schematically the main features of this apparatus.

To duplicate 30-cm thruster operation, the single hole accelerator systems were operated at beam current per hole values (corrected from Hg^+ to Ar^+ operation) and relative grid translations corresponding to different locations between the axis and periphery of a 30-cm thruster accelerator system. Accurate grid separation and translation values were ensured by fabricating the simulated 30-cm thruster grid sets from graphite to a size much larger than actually used on this thruster. As an example, the simulated grid set screen hole diameter was 12.70mm compared to a SHAG

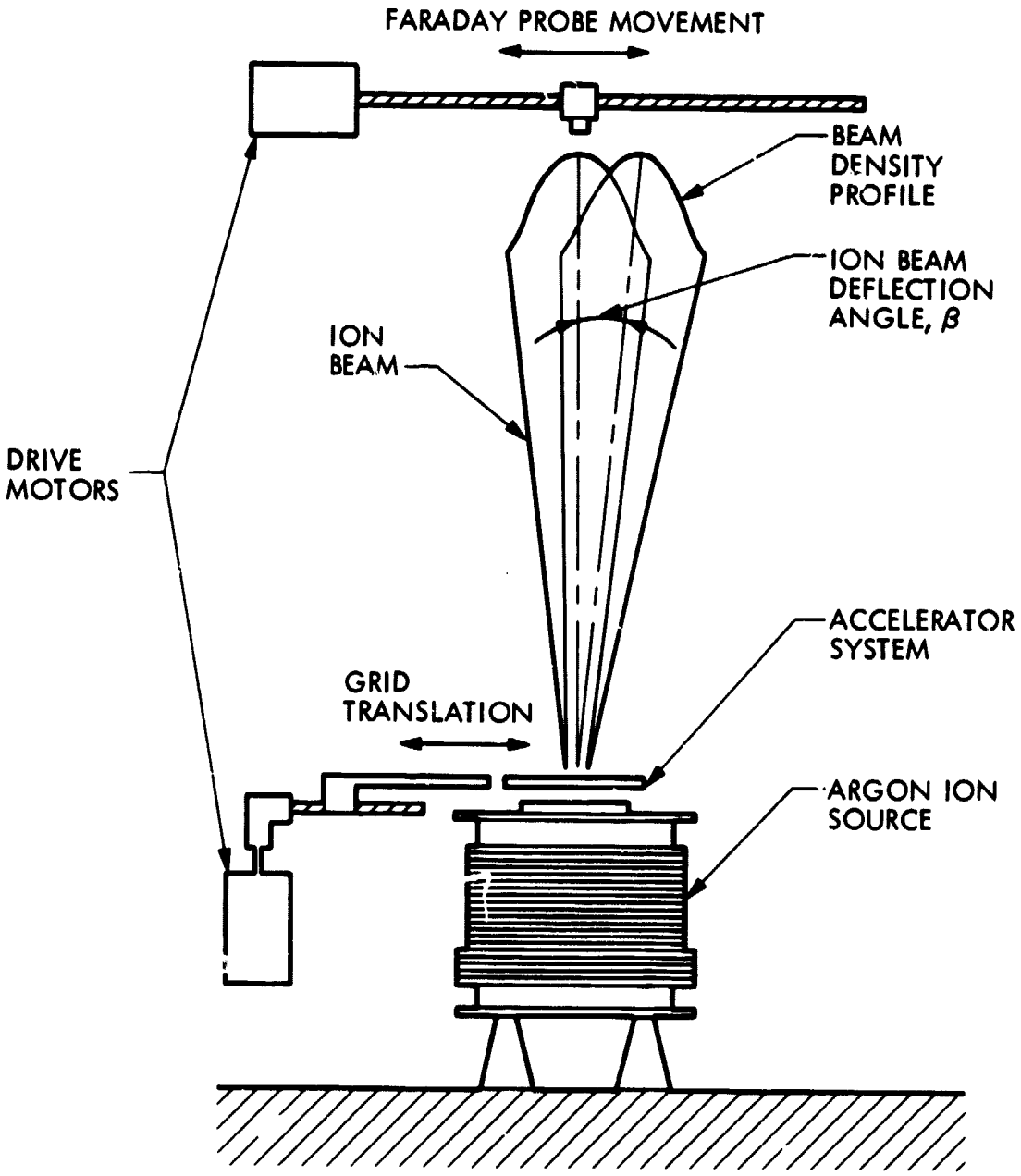

Fig. 1. Thruster Simulation Apparatus

grid set screen hole diameter of 1.905mm. Other simulated grid set dimensions were increased by an equivalent amount. Although much larger in size, these single hole grid sets still operated at the same beam current per hole and accelerating voltages as a 30-cm thruster grid set.

To determine the variation in ion current per hole across the diameter of a SHAG grid set, the plasma density profile immediately upstream of the grid set was required. Figure 2a shows the plasma density profile used for this work. This profile was derived from an ion beam Faraday probe survey close to the accelerator grid of a 30-cm thruster taken by Beattie[4]. Double ions are included in this profile which represents thruster operation at a 2.0 ampere mercury beam current level. For the test results presented in this paper all simulated 30-cm thruster operation at beam currents of 2.0 ampere and greater were assumed to have a plasma density profile identical to that shown in Fig. 2a. The effect of the non-uniform radial plasma density inherent in the 30-cm thruster discharge chamber is to produce a rather peaked distribution in the fraction of total thruster beam current emerging from the thruster grid set. Figure 2b plots this peaked beam current fraction distribution and illustrates that most of the thruster beam current originates from an annular region centered approximately 10cm from the SHAG grid set axis.

Tests with both the two and three-grid simulated 30-cm thruster grid sets were performed assuming a 0.3% grid set compensation. This value is equal to the amount of grid translation introduced during the fabrication of the dished 30-cm thruster SHAG optical system. The intent of this compensation has been to lessen the off-axis thrust loss by attempting to

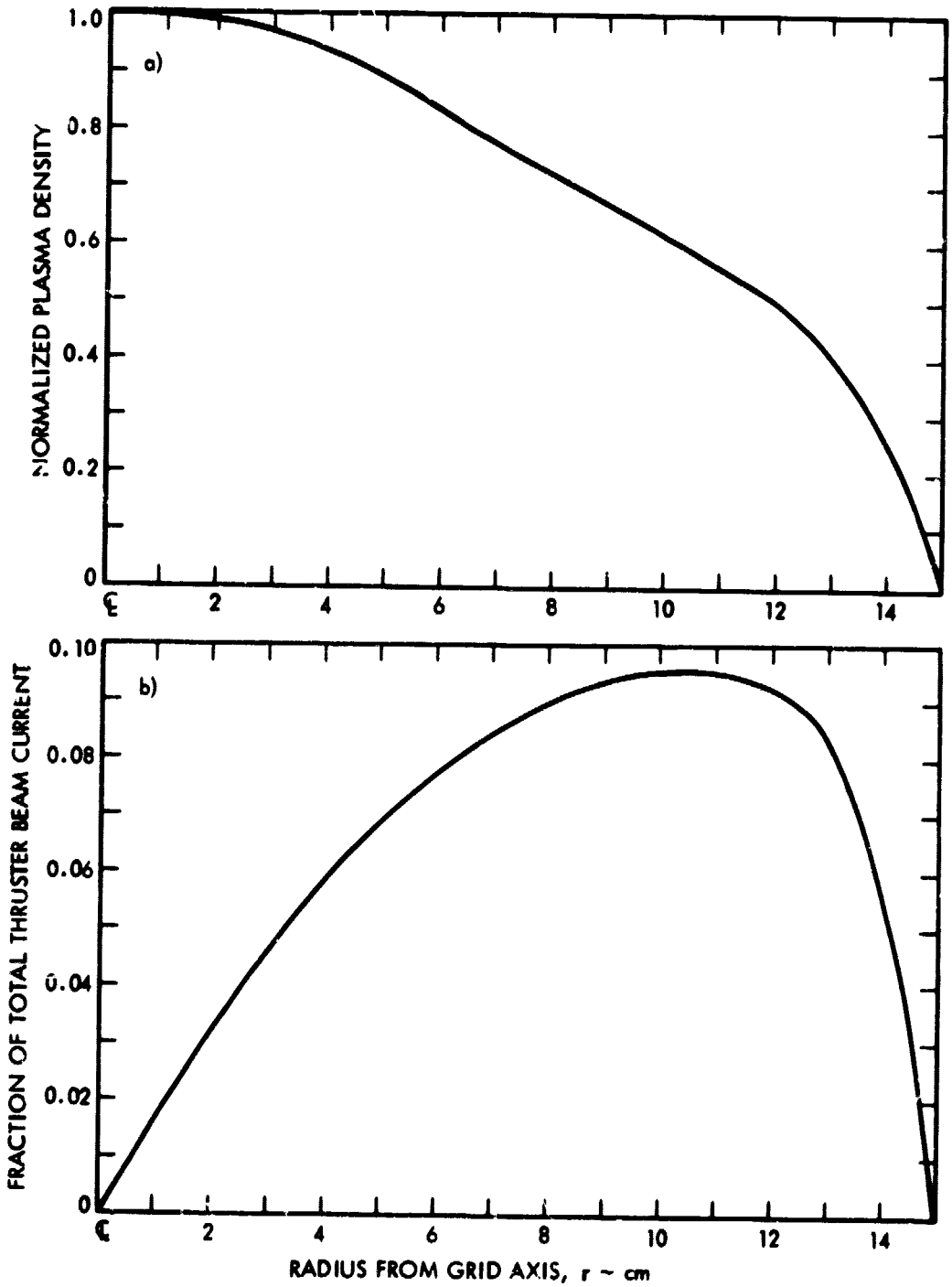

Fig. 2. a) 30-cm Thruster Plasma Density Profile
b) Grid System Beam Current Fraction

electrostatically steer the otherwise skewed ion beamlets onto a path somewhat parallel to the thruster axis. For all the results presented in this paper, the screen grid of the 30-cm thruster simulated grid sets remained centered on the ion source axis while the necessary compensation was achieved by translating either the accelerator or decelerator grids. Finally, it must be noted that during the chemical etch process used to form the holes in a set of molybdenum 30-cm thruster grids, the hole edges are not straight but are scalloped in appearance[5]. During the course of this work it was observed that under some conditions, simulated grid sets fabricated with straight edge holes exhibited noticeably larger levels of impingement current than if these same grid set geometries were fabricated with scalloped holes. Consequently, all the data in the following sections are for shaped grid set holes that are approximatley equivalent to the scalloped molybdenum thruster grid holes formed by a 50/50 chemical etch.

Two Grid Tests

For the two-grid tests, the single hole grid set non-dimensionalized accelerator system geometrical parameters were identical with those of the J-series 30-cm thruster SHAG optics system. These grid set parameters were:

$$\frac{d_a}{d_s} = 0.60$$

$$\frac{t_s}{d_s} = 0.20$$

$$\frac{t_a}{d_s} = 0.20$$

Here, d_a is the accelerator hole diameter and t_s and t_a are the screen and accelerator grid thicknesses, respectively. As previously mentioned, the simulated grid set screen hole diameter d_s was 12.70mm. Unless noted otherwise, all two-grid tests were performed at a total accelerating voltage V_T of 1420 volts, an arc discharge voltage V_D of 30 volts and a net-to-total accelerating voltage ratio R of 0.78. These parameter values represent baseline J-series 30-cm thruster operation.

Beam Deflection and Impingement

Figure 3 shows the variation in ion beamlet deflection and accelerator hole ion impingement current for the simulated 30-cm thruster SHAG single hole grid set, with 0.3% grid compensation and an equivalent 2.0 ampere Hg^+ beam current. As shown in Fig. 3, a large range of screen-to-accelerator

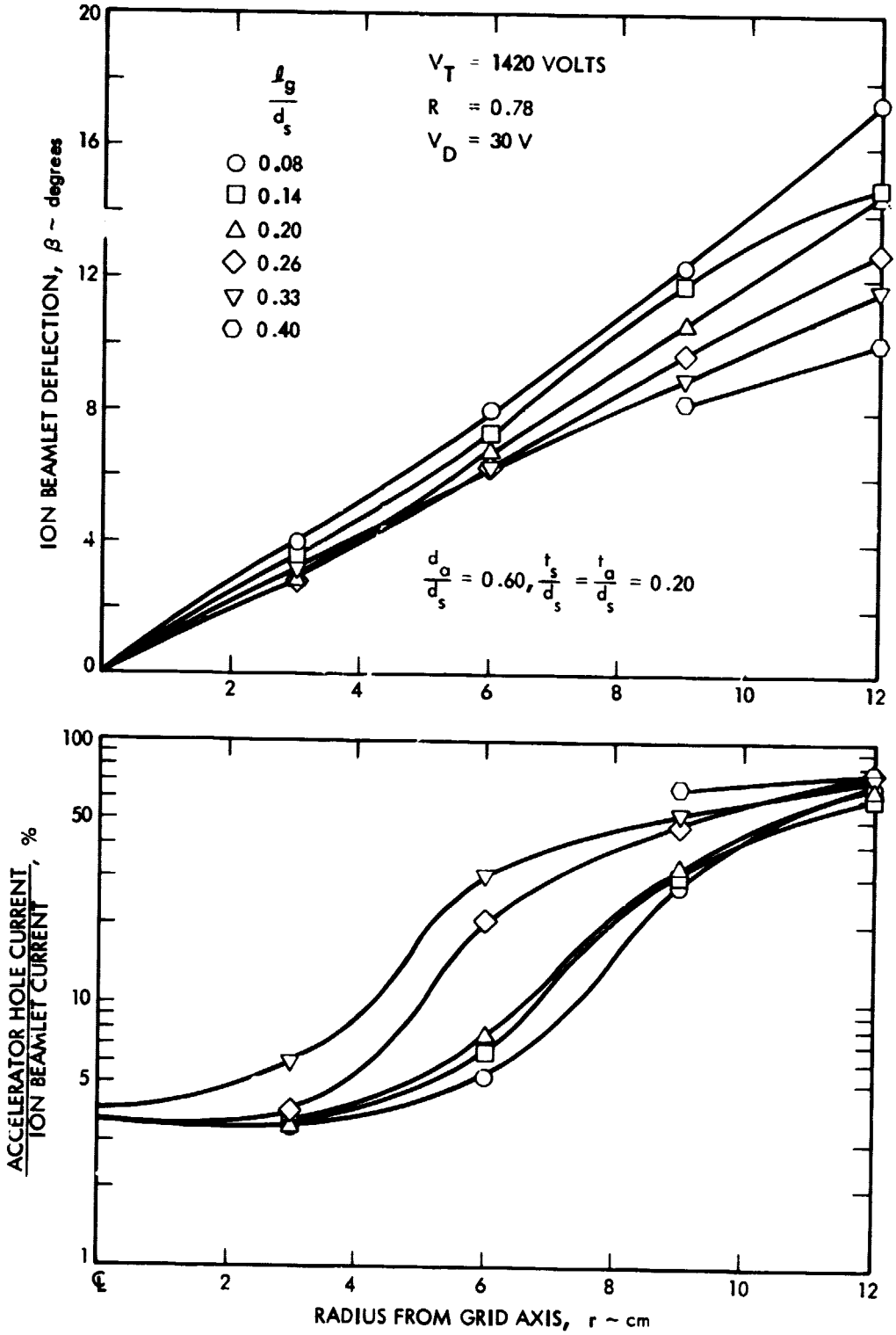

Fig. 3. Simulated SHAG Beamlet Deflection and Impingement

grid separation ratios, ℓ_g/d_s, were investigated in an effort to examine all grid gap spacing variations expected to be encountered across the diameter of a 30-cm SHAG accelerator system. The ion beamlet deflection angles recorded in Fig. 3 were determined by taking Faraday probe beam profiles at each simulated radial location and measuring the angular shift of the peak current density point from the untranslated zero radius location for each of these profiles. Inspection of Fig. 3 shows that ion beamlet deflection increases approximately linearly with linear grid translation increases (remember that 0.3% grid compensation means that at any given radial location the accelerator grid hole is positioned radially further out from the corresponding screen hole by a distance equal to 0.003 times the screen hole radial location). This linear increase in deflection angle appears to be essentially independent of beamlet current, which decreased by approximately a factor of two for the single hole grid sets in going from a simulated axial to a simulated 12cm radial grid location.

Several workers have investigated experimentally the effect of grid translation on ion beamlet deflection for multiaperture and multiple electrode accelerator systems[6-9]. The results of these studies indicate that the beam deflection angle β, for two grids with circular aperatures, varies directly as the radial grid translation Δr, and inversely as the ion emitting surface to accelerator grid separation, ℓ. A straight forward derivation by Stewart et.al[8], using the thin lens approximation of Davisson and Calbick [10], provides some physical basis for this relationship. Introducing the proportionality constant C, we may write

$$\beta = C \frac{\Delta r}{\ell} \cdot$$

Here, the ion acceleration length ℓ, is equal to the sum of the screen-to-accelerator grid separation ℓ_g, and the average distance between the downstream screen grid face and the ion emitting surface. A previous ion extraction study[11] quantifies this latter separation distance. During this study it was observed that screen grid thickness variations did not affect the average ion emitting surface location. In addition, this surface was more planar in shape than had been thought previously and different screen-to-accelerator grid separations did little to affect the location of this emitting surface. Only beam current variations were observed to substantially effect the ion emitting surface location. However, even for the beam current density variations across a 30-cm thruster, these emitting surface location changes are relatively minor. Consequently, as indicated by the data in Ref. 11, an essentially constant value of $0.3d_s$ can be ascribed to the average distance between the downstream screen grid face and the ion emitting surface. Using these expressions for the ion acceleration length ℓ, and expressing the radial grid translation in terms of the degree of grid compensation δ, and radial grid location r, the ion beam deflection angle takes on the form

$$\beta = C \frac{\delta r}{\ell_g + 0.3d_s} .$$

From Fig. 3 the constant C was evaluated to give the ion beam deflection angle, in degrees as

$$\beta = \frac{36.6\delta r}{\ell_g + 0.3d_s} . \qquad (1)$$

Although semi-empirical in form, Eq. (1) may be used to quickly obtain approximate ion beamlet deflection angles for most two-grid accelerator system geometries of interest in ion thruster applications. For

values of the net-to-total accelerating voltage ratio R, much less than the value of 0.78 used here, Eq. 1 ceases to provide reasonably accurate deflection angle predictions. This occurs because at lower R values a two-grid accelerator system really operates like a three-grid system, with the missing third grid defined by the neutralization surface located at some distance downstream of the accelerator grid. Recent two-grid translation work by Homa[9] shows the effect of R on the measured ion beamlet deflection angles. While the accelerator grid to neutralization surface separation distance does depend on the value of R, this relationship remains unspecified due to the tenuous nature of the neutralization surface. An analytical expression for this deceleration length inherent in a two-grid accelerator system has been suggested by Kaufman[12]. It was beyond the scope of the present work to incorporate such an expression into a three-grid beamlet deflection model of two-grid low R value operation.

Figure 3 also shows the variation in accelerator grid hole impingement current across the diameter of the simulated 30-cm thruster SHAG accelerator system for different grid separation values. For these curves, the accelerator grid impingement current has been expressed as a percentage of the total ion beamlet current passing through the screen and accelerator grid hole pair at the given radial location. Over the range of grid separation distances investigated direct accelerator hole ion interception increases substantially at increasing radial distances from the grid set axis. To get the implications of these results in perspective, several comments concerning the interpretation of these data must be made. First, it should be noted that the impingement current levels shown in Fig. 3 are artificially high. This is a consequence of intergrid charge exchange ion production

scaling linearly with acceleration length, while extracted ion current density scales as acceleration length squared. In going from the much smaller hole 30-cm thruster grid set to the large single hole simulated SHAG accelerator systems used for this work, charge exchange ion production becomes significant. This effect is further compounded by a minimum propellant flow needed to sustain the dilute argon plasma discharge used during this study. In addition to this charge exchange effect, which influences the baseline impingement values shown in Fig. 3, the onset of direct accelerator grid ion interception occurs very abruptly beyond a certain value of grid translation. As a result, small errors in the grid translation positioning apparatus can have a large effect on the observed simulated 30-cm thruster grid set impingment values. Also, for the sizable grid translations inherent in the 30-cm thruster SHAG accelerator system at large radial locations, small beam current per hole changes can substantially affect direct ion impingement current changes. Consequently, the absolute impingement current values observed with the simulated grid set apparatus are very dependent upon the absolute accuracy of the J-series 30-cm thruster radial plasma density profile assumed for this study. Finally, while a grid compensation value of 0.3% was used for the single hole simulated SHAG grid set tests, there is still some uncertainty as to the actual compensation value and the radial uniformity of this value in a set of hot J-series thruster optics extracting a 2.0 ampere mercury ion beam.[13]

The net result of all of the effects discussed above is that the impingement current curves shown in Fig. 3 should be thought of as depicting a qualitative trend only. The extreme sensitivity of direct accelerator grid ion interception to these cummulative effects, implies that simulated grid

set operating conditions only a few percent different from those used to obtain the results of Fig. 3 could easily show a flat unchanging impingement current level with grid set radial location.

Recent work indicates that a 30-cm thruster SHAG accelerator system operating at a 2.0 ampere beam current level has a grid gap spacing that varies linearly from $\ell_g/d_s = 0.227$ at the thruster axis to $\ell_g/d_s = 0.267$ at the grid set periphery [14]. Using this information and the data presented in Fig. 3, the simulated grid set apparatus estimates of the 30-cm SHAG grid set beamlet deflection and accelerator hole impingement as a function of radial grid set location were determined. Figure 4 illustrates these trends. The impingement current variation shown in Fig. 4 indicates that the 30-cm SHAG optics system is over compensated. As a result, beyond a radial distance of about 5cm the screen and accelerator grid translations are increasing faster than the beamlet diameters passing through the accelerator holes are decreasing due to the reduced plasma density and ion beamlet current. With this design error, the 30-cm SHAG grid set will experience excessive accelerator grid impingement currents over the outer annular grid set area as thruster operation beyond approximately 2.0 amperes is attempted. This situation is doubly unfortunate because the major fraction of total thruster beam current originates in the central portion of this impingement plagued region of the SHAG accelerator system (Fig. 2b). Finally it should be noted that the error bands on the deflection angle and impingement current curves in Fig. 4 are for the simulated grid set apparatus random electrical and mechanical uncertainties only. These error bands pertain to all the data presented in this paper. Because of the cummulative effects described earlier, the impingement current error band is not intended to encompass actual 30-cm SHAG grid set operation.

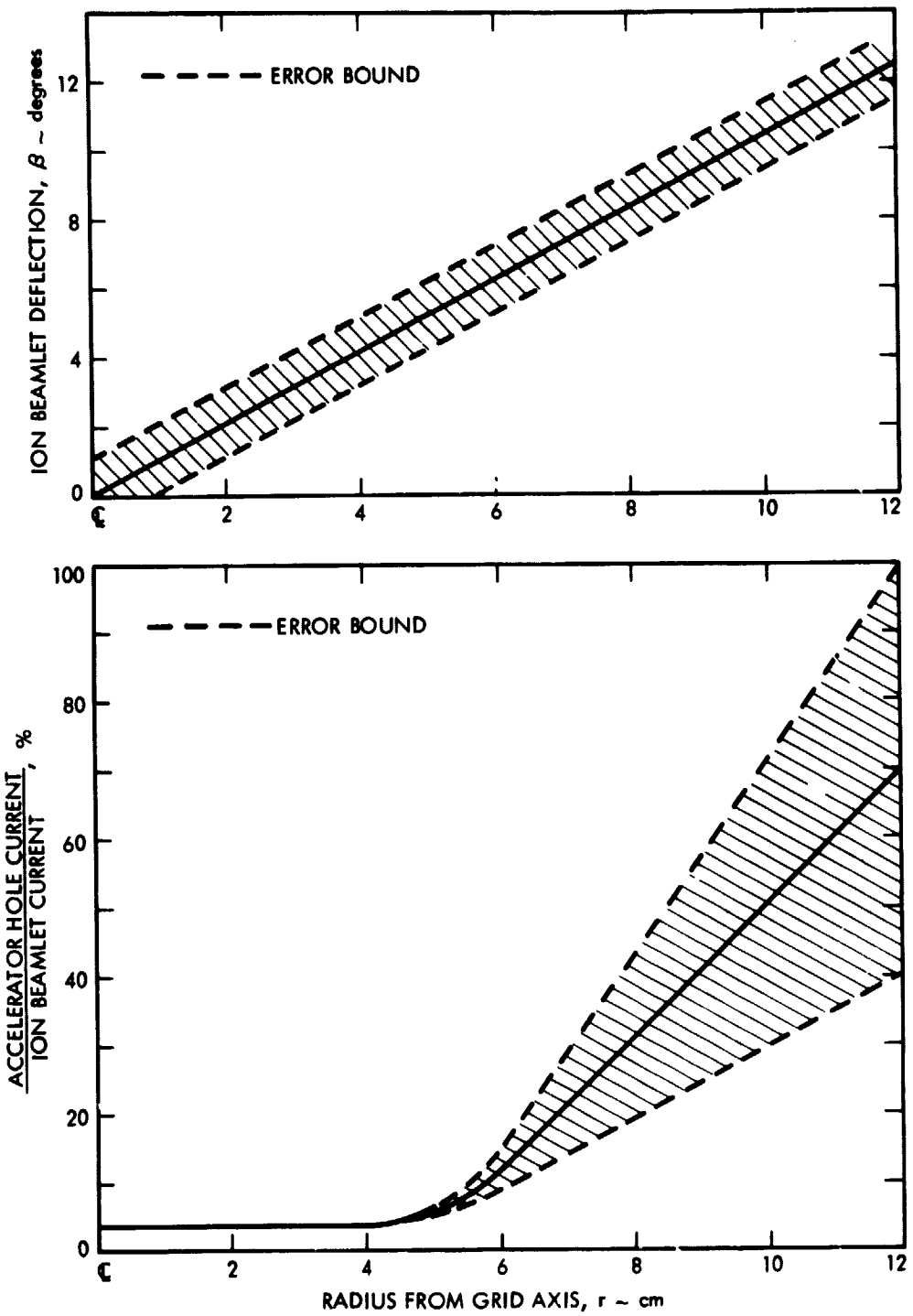

Fig. 4. Simulator Predictions of 30-cm Thruster Beamlet Deflection and Impingement

Uniform Perveance Limit Grid Set

From the results presented in Figs. 3 and 4 it became apparent that significant beam current gains might be possible if the J-series 30-cm thruster were fitted with a minimally compensated accelerator system which reached its perveance limit uniformly across the grid set area. To assist in the design of such an accelerator system, a semi-empirical model was formulated to describe the anticipated accelerator system behavior. As a starting point in the model development, the radial plasma density distribution of Fig. 2a was assumed for the 30-cm thruster at higher levels of beam current operation. The second piece of required information was the maximum accelerator system gap electric field stress, this maximum stress being experienced by the grid set center line hole pair. Beattie and Poeschel[1] have demonstrated reliable 30-cm thruster accelerator system operation at a cold average gap field stress of 5.8 KV/mm. A central hole gap field stress E, of 5.0 KV/mm was selected for the model calculations. Because of the peaked plasma density profile (Fig. 2a) and low beam current fraction contributed by the central grid holes (Fig. 2b), the model predictions are not overly sensitive to the central hole gap field stress choice.

To complete the necessary model input information, a series of curves describing the ion beam divergence angle α, as a function of the normalized perveance per hole NP/H, were derived from previous ion optics work[15]. These curves are shown in Fig. 5a. In this figure, the line of maximum normalized perveance per hole (NP/H_{max}) pertains to that point at which excessive accelerator grid impingement currents (for a non translated grid set) prevent further beam current increases. Similarly, the maximum safe operating limit line references that beam current beyond which further

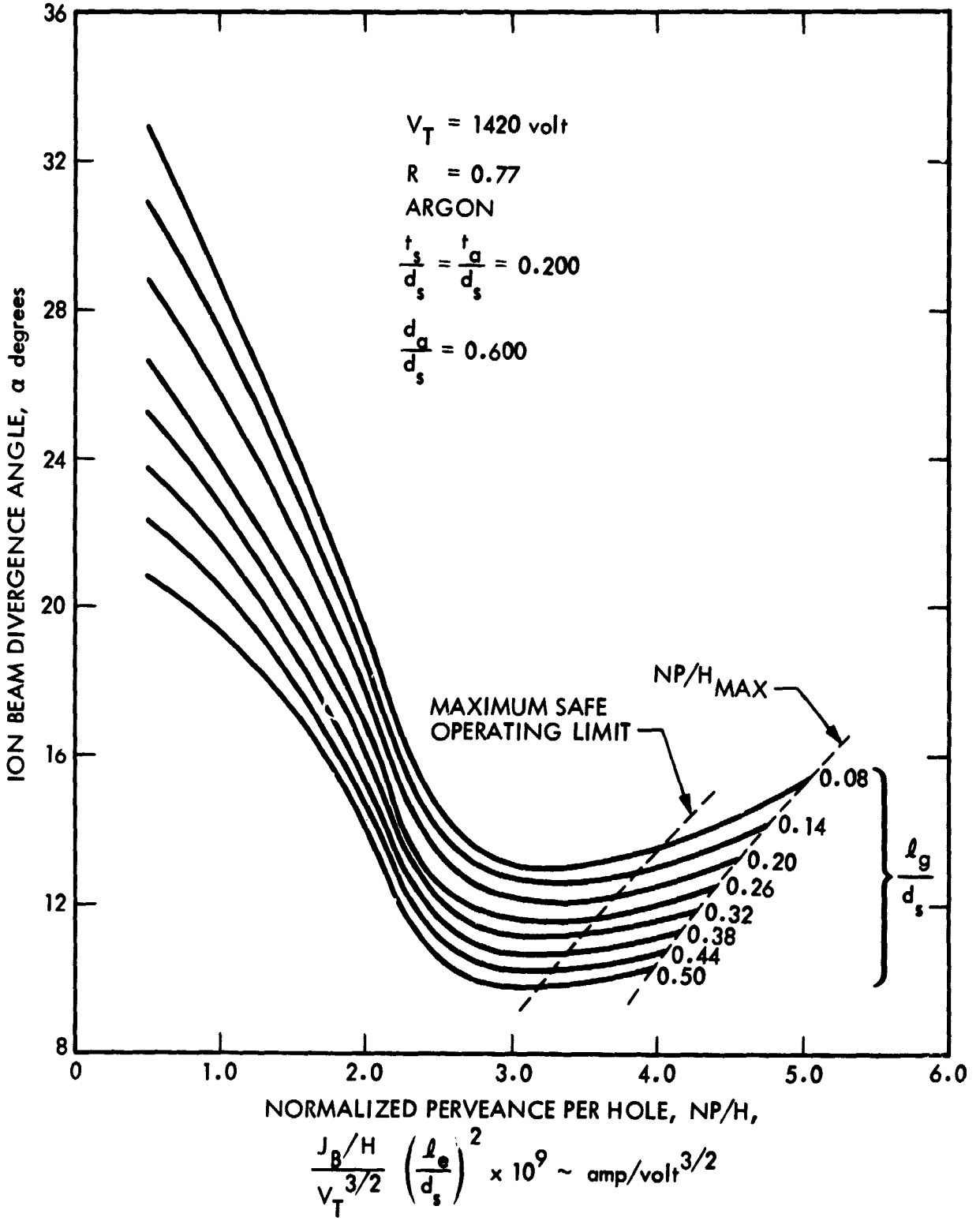

Fig. 5a. Generalized SHAG Divergence Angle and Normalized Perveance Characteristics

beam current increases no longer result in a linear impingement current increase because of the onset of direct accelerator grid ion interception. Figure 5b plots the maximum safe normalized perveance per hole value against the accelerator system grid separation ratio. It should be noted that argon ion normalized perveance per hole values have been used in Fig. 2 because the simulated 30-cm thruster grid set apparatus uses an argon plasma.

From Fig. 5b a straight line equation was determined to be a good approximation to the curve shown. This equation and Childs'[16] one-dimensional space charge limited ion flow equation are written below:

$$NP/H = -2.03\times10^{-9}(\ell_g/d_s) + 4.14\times10^{-9} \qquad (2)$$

$$NP/H = \frac{J_B/H}{V_T^{3/2}}\left((\ell_g/d_s)^2 + 0.25\right). \qquad (3)$$

Here, J_B/H is the grid set beam current per hole (A/m^2) and V_T is the total ion accelerating voltage. Equations (2) and (3) describe the operation of a SHAG accelerator system assuming no grid translation and a total accelerating voltage of 1420 volts. These equations were solved for NP/H and ℓ_g/d_s given the calculated grid set centerline beam current per hole, J_B/H. To calculate this latter parameter, the axial grid separation ℓ_g, was found from the field stress relation

$$E = \frac{V_I}{\ell_g} = \frac{1420}{\ell_g} = 5\times10^3 \text{ v/m}. \qquad (4)$$

From Eq. (4) the axial grid set separation ratio was $\ell_g/d_s = 0.15$. Using this number in Eq. (2) to solve for the corresponding safe maximum NP/H value and then substituting the result in Eq. (3), gave an argon ion center

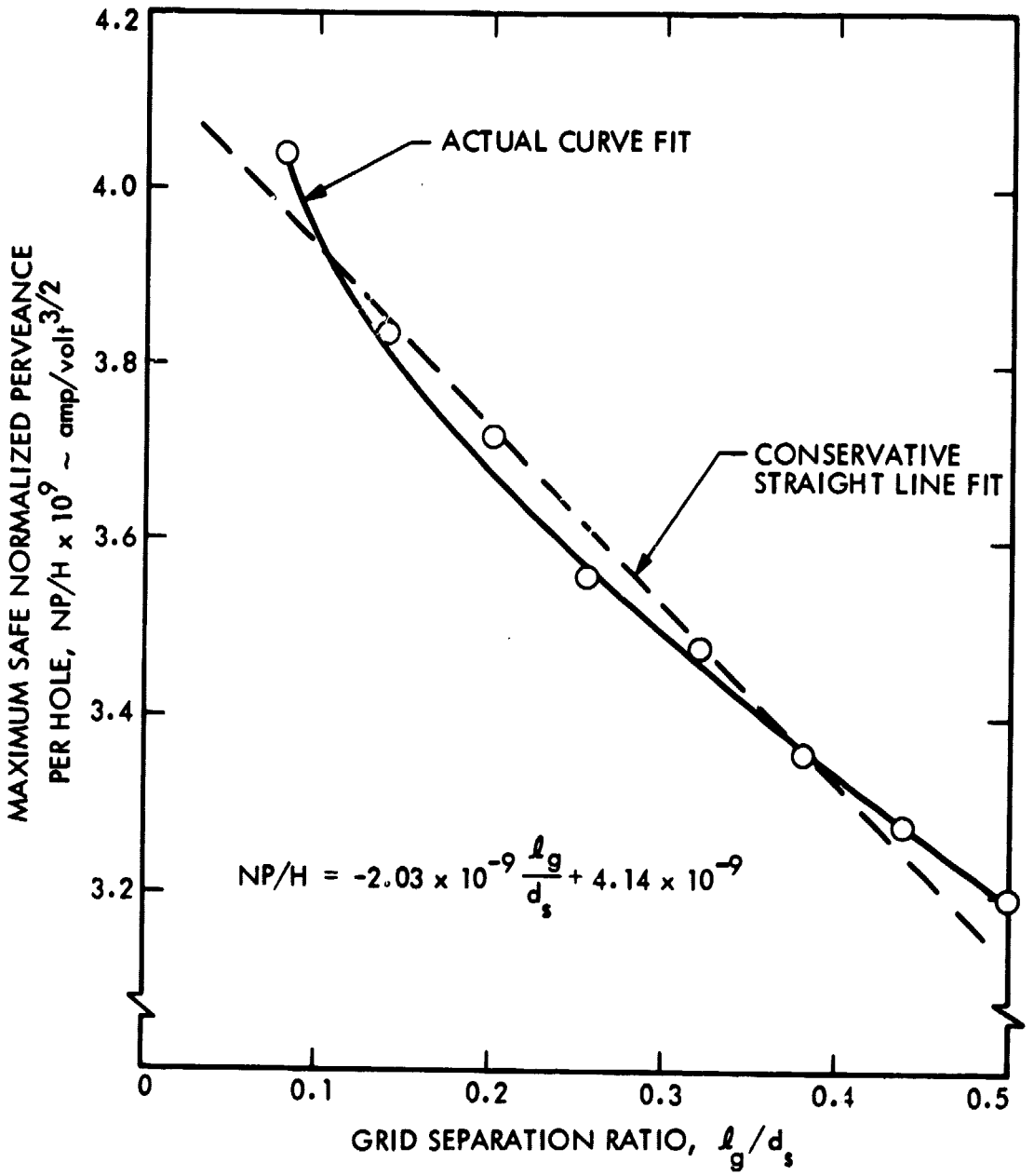

Fig. 5b. Predicted Limits of SHAG Accelerator System Operation

line J_B/H of 0.76 mA. In solving Eqs. (2) and (3) for NP/H and ℓ_g/d_s, subsequent J_B/H values were evaluated by modifying the 0.76 mA value by the plasma density distribution in Fig. 2a.

Table 1 documents the calculated solutions to Eqs. (2) and (3) for the initial conditions discussed above. Included in Table 1 is the average ion beam divergence angle, per annular grid segment, as described by Fig. 5a. From these model predictions it was apparent that a 50% mercury beam current increase (from 2.0 to 3.0 ampere) was possible as a consequence of relatively minor changes to the present 30-cm thruster SHAG accelerator system design. These modifications include a carefully prescribed grid spacing variation across the grid diameter and grid compensation sufficient to ensure all beamlets emerge normal to the dished accelerator system surface.

To test the model predictions for uniform perveance limited grid set operation, a series of experiments were performed to verify the maximum safe ion current per hole values for this modified 30-cm thruster SHAG accelerator system geometry. Figure 6 shows the results of these experiments, which covered accelerator system total voltage operation from 1420 to 2500 volts. Comparison of the model predictions in Table 1 with the V_T = 1420 volt curve in Fig. 6, shows good agreement with the simulated accelerator system experimental results. The only significant discrepancy between these results was for the center line grid set separation necessary to obtain a maximum safe beam current per hole J_B/H, of 0.76 mA. In the experiment, an axial grid set separation ratio of ℓ_g/d_s = 0.20 was actually required rather than the value of ℓ_g/d_s = 0.15 predicted by the model. The consequence of this difference is that the center line electric field stress for the modified

Table 1: Projected Uniform Perveance Limit
Grid Set Performance (Argon)

Annular Region Radius (cm)	Holes in Region	Current per Hole (mA)	ℓ_g/d_s	NP/H $\times 10^9$ (amp/volt$^{3/2}$)	α Divergence (degrees)
0.5	67	0.760	0.144	3.847	12.8
1.5	202	0.760	0.144	3.847	12.8
2.5	337	0.751	0.152	3.832	12.7
3.5	472	0.732	0.167	3.801	12.5
4.5	607	0.700	0.192	3.751	12.3
5.5	742	0.657	0.224	3.685	12.0
6.5	877	0.617	0.254	3.625	11.7
7.5	1012	0.573	0.287	3.558	11.4
8.5	1146	0.533	0.318	3.495	11.1
9.5	1281	0.490	0.352	3.425	10.8
10.5	1416	0.447	0.389	3.351	10.6
11.5	1551	0.406	0.426	3.275	10.3
12.5	1686	0.354	0.479	3.169	9.9
13.5	1821	0.260	0.595	2.933	9.1
14.5	1956	0.108	0.931	2.249	7.1

Total Ar^+ current = 6.619 ampere

Equivalent Hg^+ current = 2.955 ampere.

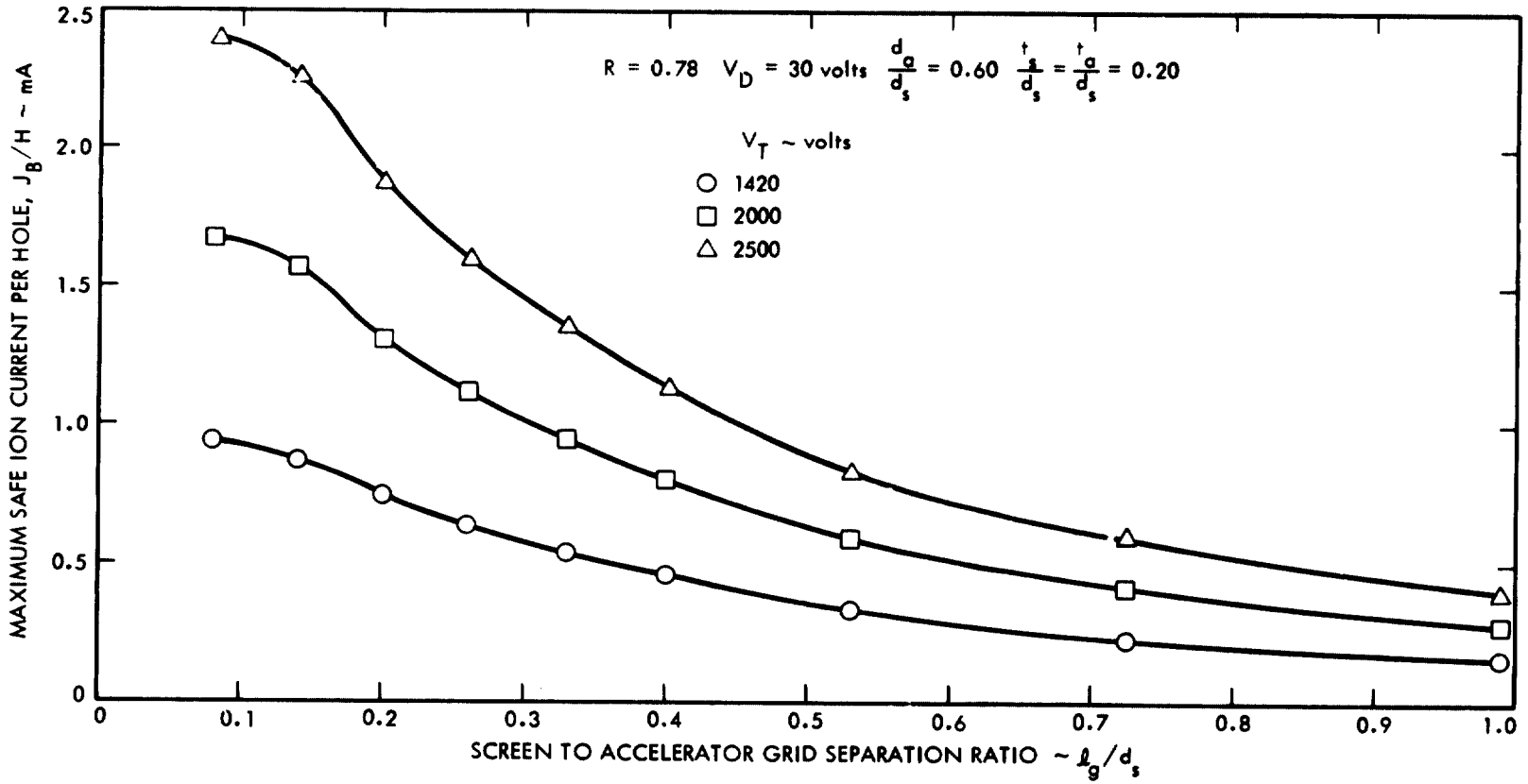

Fig. 6. Experimental Verification of Uniform Perveance Grid Set Operating Limits

SHAG accelerator system is only 3800 volts/mm rather than the 5000 volts/mm originally specified for the model. This lowered peak electric field stress requirement is not much different from the peak stress of 3300 volts/mm recently determined for the present 30-cm thruster SHAG accelerator system.[14]

From the modified SHAG accelerator system beam current per hole test results shown in Fig. 6, a plot of total grid set beam current as a function of total accelerating voltage was determined. Figure 7 plots this relationship and compares the resultant beam current trend (corrected from argon to mercury ions) with data from Rawlin[3] for 30-cm thruster operation with a standard SHAG accelerator system. An essentially 1.0 ampere mercury ion beam current increase is observed for the uniform perveance limited grid set over the standard SHAG grid set for the total accelerating voltage range investigated. This result is important because it shows that significant 30-cm thruster beam current gains, for the same specific impulse value, can be realized with the modified SHAG accelerator system design proposed here.

It is interesting to note that although the ion beamlets in the uniform perveance limited grid set design emerge perpendicular to the dished grid set curved surface, the thrust loss incurred by doing this is small. Figure 8 plots the 30-cm thruster modified SHAG accelerator system thrust loss for these off-axis ion trajectories as a function of the grid set radius of curvature. To calculate these thrust loss factors, the beamlet divergence angle for each radial grid set location shown in Table 1. was converted into the corresponding beamlet thrust loss factor by using a generalized conversion curve derived during an earlier study[17]. The appropriate numerical integrations were then performed using these individual beamlet thrust loss

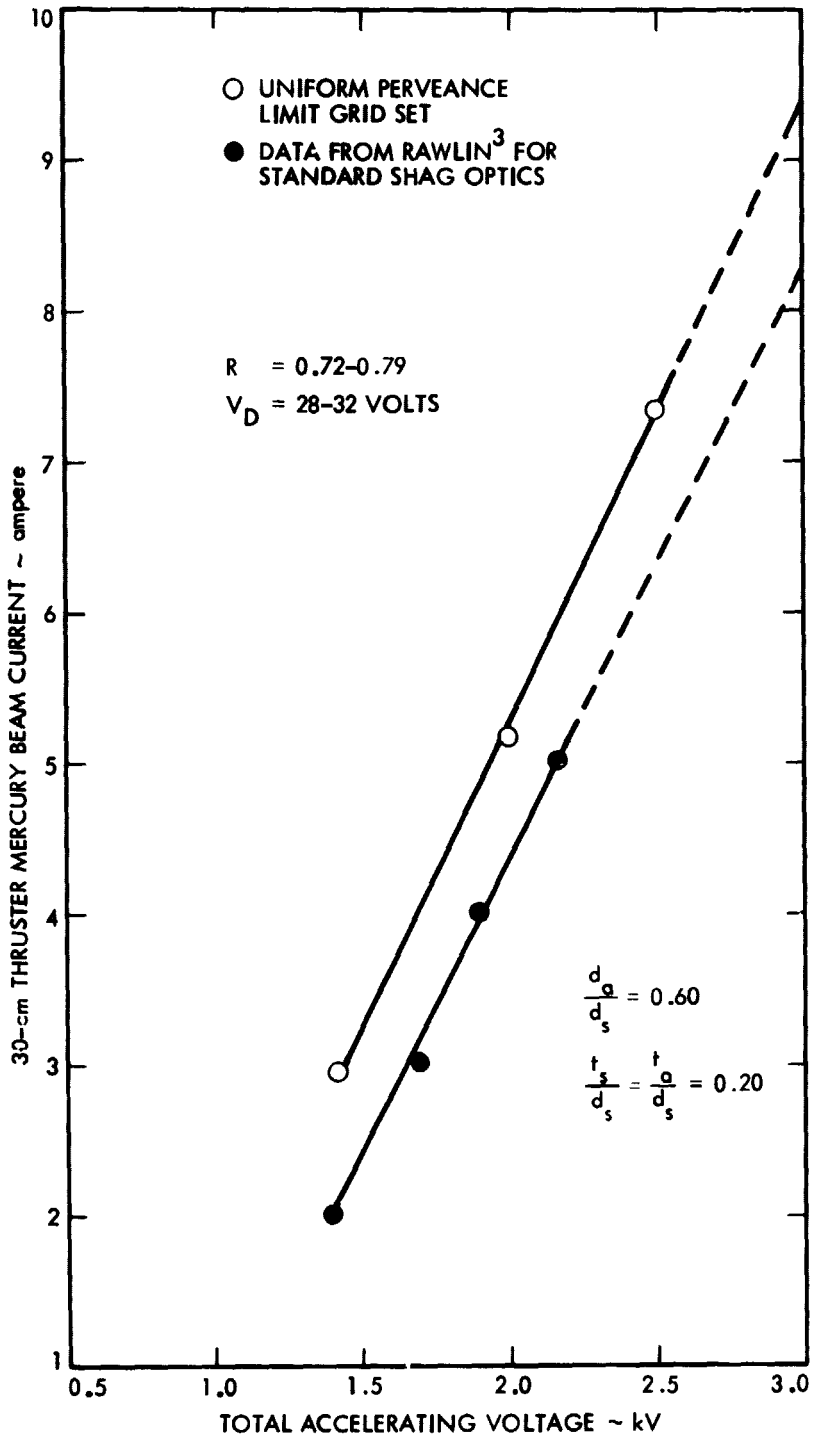

Fig. 7. Comparison of Uniform Perveance Limited Grid Set and SHAG Grid Set Performance

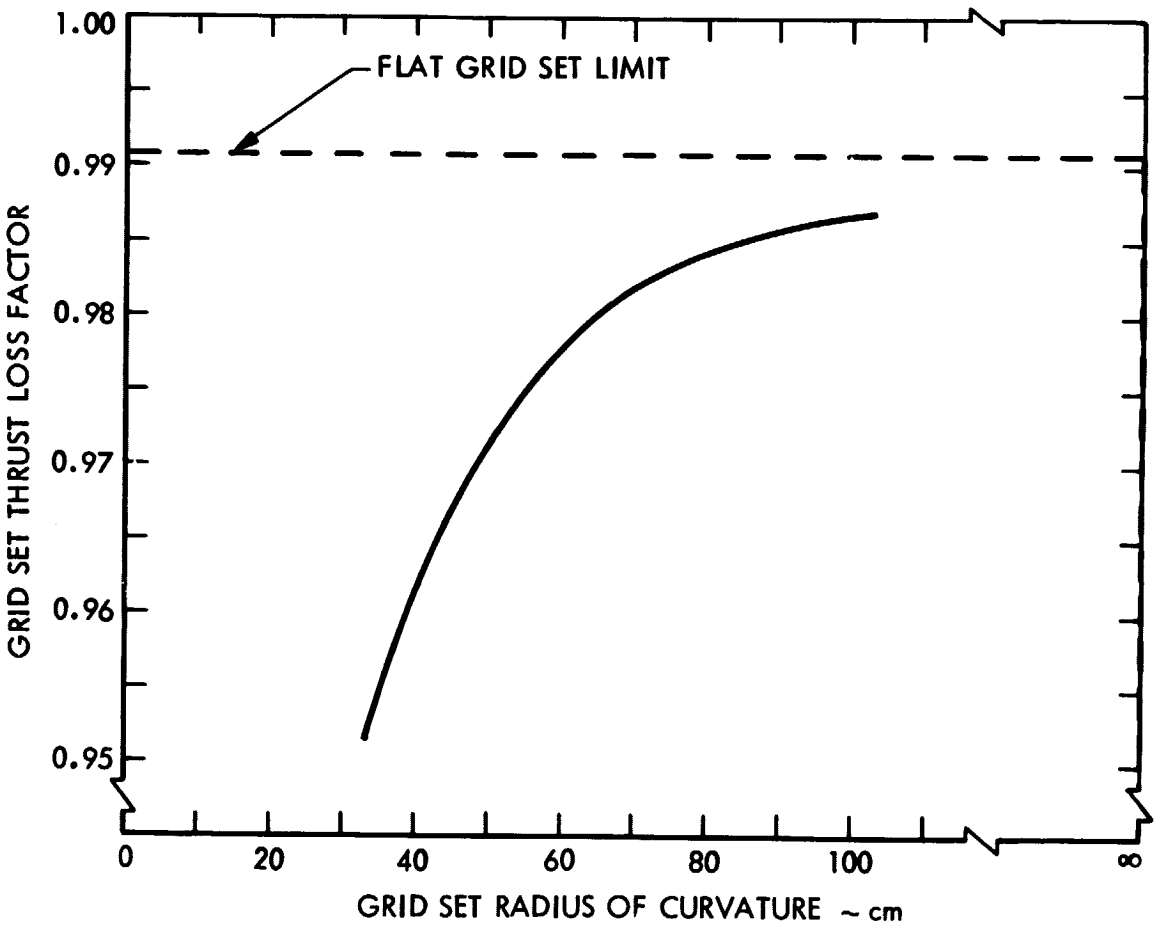

Fig. 8. Uniform Perveance Grid Set Thrust Loss

factors, the grid set beam current variation and the inherent geometrical thrust loss due to the curved accelerator system surface. The results of these integrations determine the whole grid set thrust loss factors shown in Fig. 8. Inspection of this figure shows that for a modified SHAG accelerator system radius of curvature of approximately 60 cm, the thrust loss factor is only about 1% less than the flat grid asymptotic value of 0.9907. It should be noted that above about 1500 volts this result is independent of accelerator system total voltage operation.[15]

While taking the data contained in Fig. 6 to derive the performance trends shown in Figs. 7-8, the maximum amount of grid translation induced beamlet deflection for the modified SHAG accelerator system was determined. The results of these beam deflection measurements are shown in Fig. 9. For these data, the maximum permissible beamlet deflection was defined as that amount of grid translation which increased the prevailing accelerator grid hole ion impingement current by ten percent. From Fig. 9 it is apparent that the small beam deflection which actually occurs (approximately 1.5^{o}) means grid translation is not a worthwhile pursuit in the uniform perveance limited grid set design. Inherent in the results presented in Fig. 9 are values of the maximum off-axis grid translation error that can be tolerated by the uniform perveance limited SHAG grid set design. This maximum grid translation error can be evaluated by determining the β value for the ℓ_g/d_s value in question from Fig. 9, then entering Fig. 3 with these values of β and ℓ_g/d_s and evaluating the translation error Δr by multiplying the implied grid set radial location by the compensation factor 0.003.

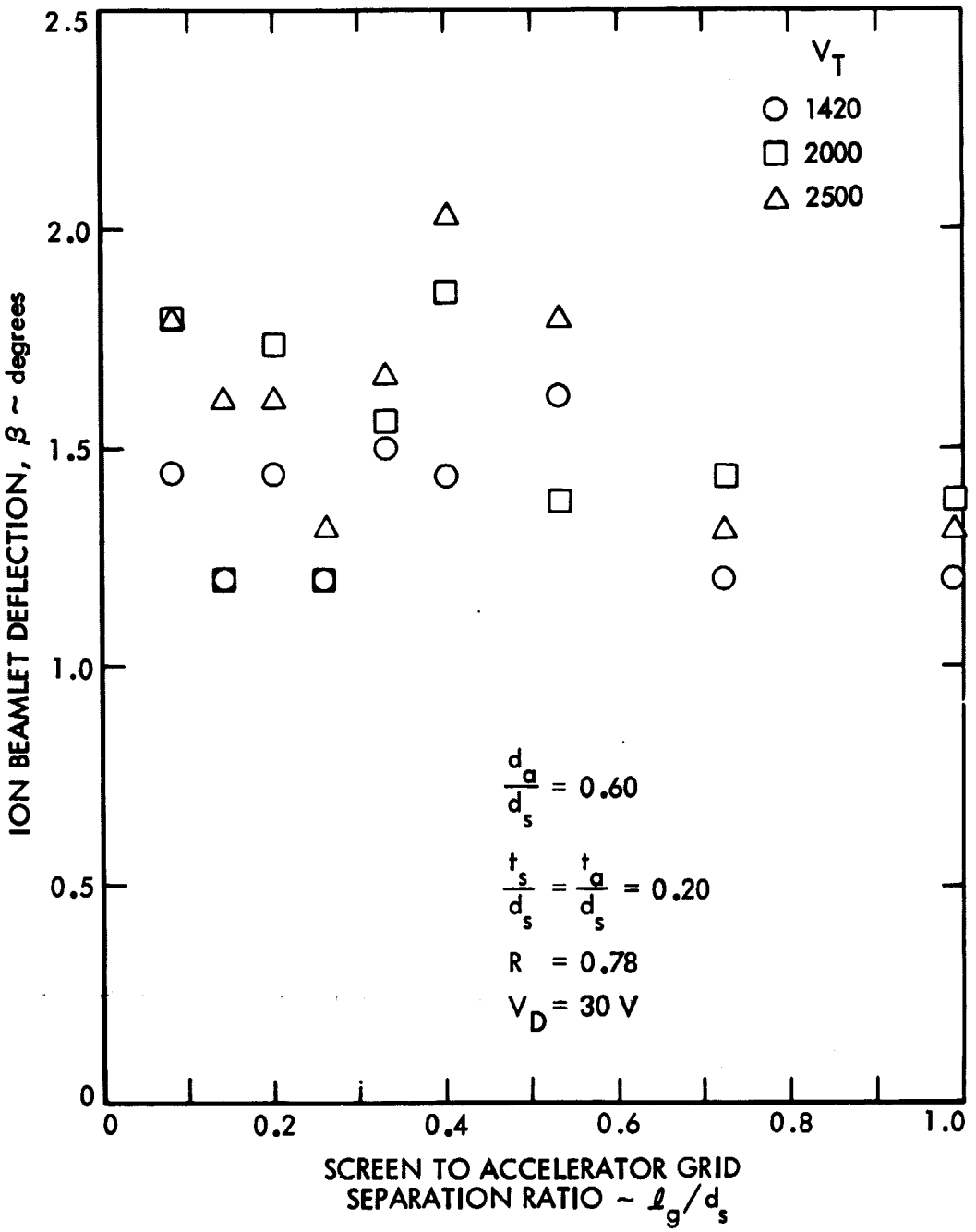

Fig. 9. Uniform Perveance Grid Set Beamlet Deflection Capability

Three Grid Tests

For the three-grid tests the simulation apparatus single hole grid sets had screen and accelerator electrodes with a non-dimensionalized accelerator hole diameter ratio d_a/d_s, of 0.6, and a screen grid thickness ratio t_s/d_s, and accelerator grid thickness ratio t_a/d_s, of 0.20. A previous three-grid ion beam divergence study[17] had indicated that minimum beam divergence angles, minimum grid impingement currents and maximum beam currents were achieved for specific decelerator grid geometry values. Those values which optimized three-grid performance, for the above screen and accelerator grid parameters, were a decelerator grid hole diameter ratio d_d/d_s of 0.80, an accelerator-to-decelerator grid separation ratio ℓ_d/d_s of 0.18 and a decelerator grid thickness ratio t_d/d_s of 0.20. All three-grid operation was with the screen and accelerator hole axis aligned. Beam deflection tests were performed by translating the decelerator grid only.

Beam Deflection and Impingement

Figure 10 shows the variation in ion beamlet deflection and decelerator hole ion impingement current for the previously described three-grid accelerator system as a function of variations in the screen-to-accelerator grid separation ratio ℓ_g/d_s, and the net-to-total accelerating voltage ratio R. For these data, the single hole grid set simulated a 30-cm thruster three-grid accelerator system, operating at an equivalent 2.0 ampere mercury beam current, with the screen and accelerator grid holes coaxially aligned and with 0.3% decelerator grid compensation. It should be noted that to achieve beamlet deflection in the same direction, the decelerator grid compensation was

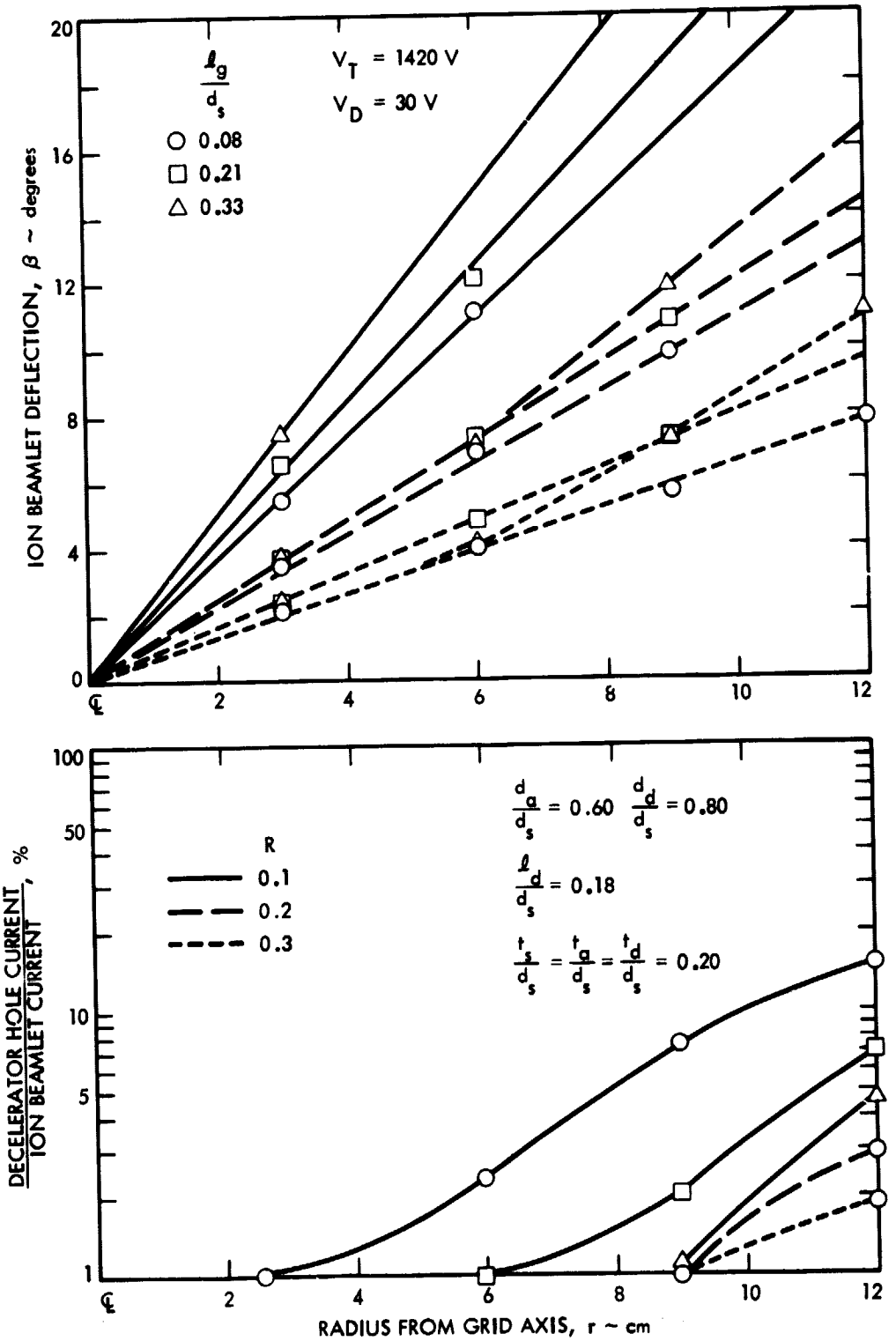

Fig. 10. Simulated Three-Grid Beamlet Deflection and Impingement Current Characteristics

opposite in sign to the accelerator grid compensation used for the two-grid tests discussed earlier. This change in effect results from the attractive forces acting on an ion as it approaches an accelerator grid in contrast to the repulsive forces acting on an ion as it approaches a decelerator grid.

Inspection of Fig. 10 shows that large beam deflection angles are obtainable by decelerator grid translation alone and that beam deflection increases with decreasing values of the net-to-total accelerating voltage ratio R. Comparing Figs 10 and 3, it is apparent that comparable amounts of beam deflection may be achieved with either two or three-grid accelerator systems. However, the results presented in these figures also illustrate that for a common grid compensation value of 0.3%, beam deflection by decelerator grid translation does not lead to excessive impingement currents on the decelerator grid. Although not shown in Fig. 10, the accelerator hole ion impingement current was approximatley 4% of the ion beamlet current across the 30-cm thruster simulated three-grid set radius. This value represented the baseline pressure induced impingement level of the simulated grid set and was to be expected, since the screen and accelerator grid holes remained coaxially aligned across the thruster radius.

A comprehensive theoretical treatment of beamlet steering by grid translation of three-grid accelerator systems has been presented by Conrad.[18] Although primarily derived for neutral beam injector ion source accelerator systems, the results are quite general in nature and with appropriate variable re-definition can be applied to the accelerator systems studied here. For beamlet steering resulting from decelerator grid translation only, Conrad shows that the ion beamlet deflection angle β, is expressed by the following relation

$$\beta = \frac{180\left(\frac{R-1}{R}\right)}{4\pi(\ell_d+0.5t_a+t_d)}\left[1-\frac{\frac{8}{27}\left(\frac{\ell_d+0.5t_a+t_d}{0.3d_s+\ell_g+0.5t_a}\right)^2\left(2R^{-3}-3R^{-5/2}+R^{-3/2}\right)}{\left(\frac{1-R}{R}\right)^3}\right]\Delta r. \quad (5)$$

Figure 11 plots the ion beamlet deflection angle and decelerator and accelerator hole ion impingement current variations for the simulated 30-cm thruster three-grid accelerator system, assuming the screen and accelerator grid separation varied from $\ell_g/d_s = 0.227$ at the thruster axis to $\ell_g/d_s = 0.267$ at the grid set periphery. Also plotted in Fig. 11 are the beamlet deflection angle predictions for this accelerator system calculated using Eq. (5). As can be seen from this figure, agreement between the experimental results and the deflection angle predictions of Eq. (5) is good at moderate R values but becomes poor for very low values of R.

Uniform Perveance Limited Operation

A series of experiments were performed to determine the amount of beamlet deflection a translated decelerator grid could produce if it were mated to the uniform perveance limited SHAG grid set design presented earlier. Figure 12 shows the results of these tests. To obtain these results the simulated 30-cm thruster three-grid accelerator system was operated at the maximum safe ion current per hole values defined by Fig. 6. In addition, the maximum permissable beamlet deflection was defined as that amount of decelerator grid translation which increased the prevailing decelerator grid impingement current ten percent. From Fig. 12 it is apparent that a decelerator grid may be placed downstream from the uniform perveance limited SHAG accelerator system and that, at low R values significant decelerator grid translation induced

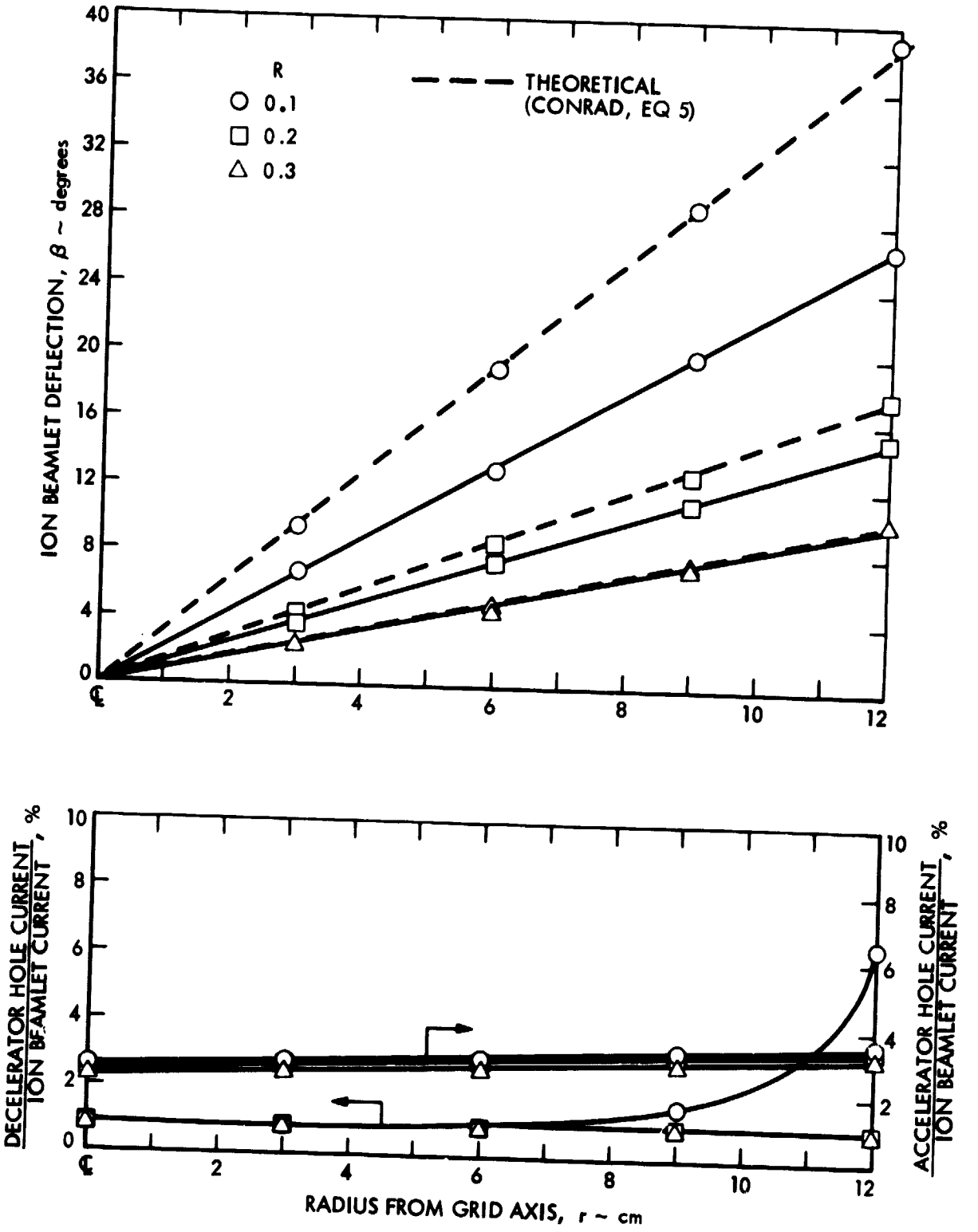

Fig. 11. Simulator Predictions of a Three-Grid 30-cm Thruster

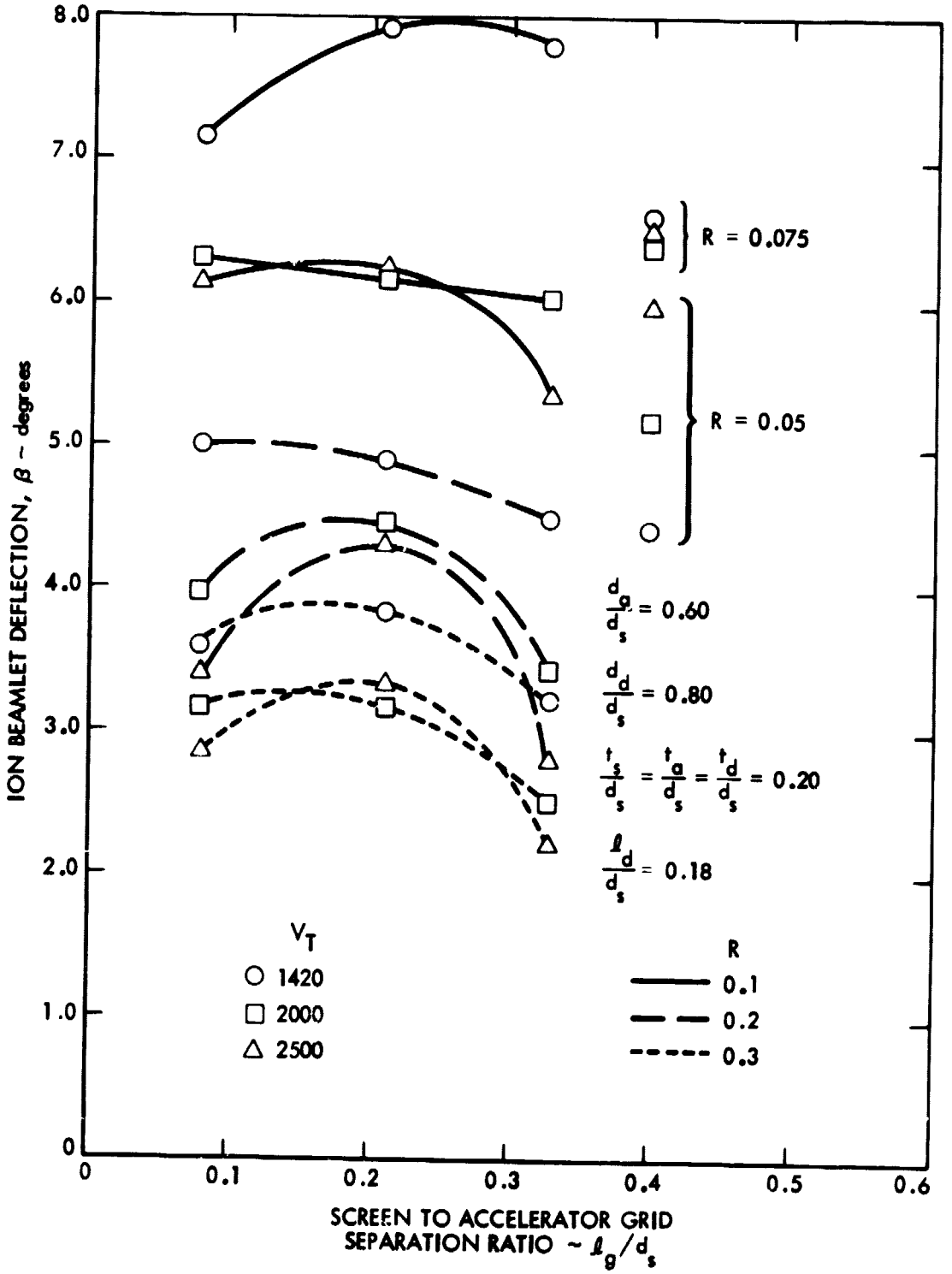

Fig. 12. Uniform Perveance Three-Grid Set Beamlet Deflection Capability

beam deflection can be realized. The amount of decelerator grid translation inherent in the results shown in Fig. 12 may be determined by substituting these ion beam deflection angles into Fig. 10, then changing the indicated radial grid locations to the corresponding values of decelerator grid translation by multiplying by the compensation factor 0.003. During this study it was observed that for identical values of grid translation, total voltage changes did not change the measured ion beamlet deflection angle.

In an effort to pursue the lower R value (or specific impulse) limits of three-grid ion thruster operation, a few beamlet deflection tests at net-to-total accelerating voltage ratio values of R = 0.075 and 0.05 were examined; these tests are also documented in Fig. 12. It is interesting to note that while very low R value grid system operation was possible, the maximum safe beam current levels before excessive accelerator grid impingement currents developed were somewhat less than those values indicated in Fig. 6. In addition, the amount of beamlet deflection attainable at these very low R values was not as great as might have been assumed from the trends of the other data presented in Fig. 12. It is thought that at these very low ion energy levels, electric field abberations, caused by mechanical imperfections in the accelerator system and by slight grid miss-alignment errors, can result in off-axis ion velocity components which are no longer negligible. These effects result in a smearing of trajectories as the ions pass through the accelerator system with subsequent poorer beam quality and earlier onset of significant direct accelerator hole and decelerator hole ion interception. Finally, it should be mentioned that at very low R values and high values of the total accelerating voltage V_T, the accelerator-to-decelerator grid electric field stress can be excessive.

As an example, for R = 0.05, V_T = 2500V, ℓ_d/d_s = 0.18 and a screen hole diameter d_s, of 1.905mm, the field stress is approximately 7.0 KV/mm.

Summary

The results of a detailed study of two and three-grid accelerator systems for high power 30-cm thruster operation has been presented. An excessive accelerator grid ion impingement current condition with the present 30-cm thruster SHAG accelerator system was identified as being caused by overcompensation of this grid set. An alternate two-grid accelerator system design for this thruster was proposed to overcome this probelm while providing substantial thruster performance gains. During the course of developing this alternate grid set design it was shown that, with a correctly matched dished two-grid accelerator system, electrostatic beamlet steering is not necessary to reduce off-axis ion thrust loss. This modified SHAG accelerator system design was further extended to include a decelerator grid for successful high power low R 30-cm thruster operation. At very low R values it was shown that electrostatic beamlet steering by decelerator grid translation only is significant.

Although the results of this work were applied specifically to a J-series 30-cm thruster, they are quite general in nature and may be used to evaluate the performance of ion source discharge chambers with more uniform plasma density profiles. It is felt that the large non-uniformity of the present 30-cm thruster discharge chamber plasma significantly lowers the thrust potential of this diameter ion engine.

Acknowledgment

The author wishes to thank Vincent Rawlin for several helpful discussions throughout the course of this work.

The research described in this paper was carried out at the Jet Propulsion Laboratory, California Institute of Technology, and was supported by NASA Lewis Research Center under Contract NAS7-918, Task Order RE-65, Ammendment 399.

References

1. Beattie, J.R. and Poeschel, R.L., "Extended Performance Thruster Technology Evaluation", AIAA Paper No. 78-666, April 1978.

2. Rawlin, V.K. and Hawkins, C.E., "Increased Capabilities of the 30-cm Diameter Hg Ion Thruster", AIAA Paper No. 79-0910, May 1979.

3. Rawlin, V.K., "Extended Operating Range of the 30-cm Ion Thruster with Simplified Power Processor Requirements", AIAA Paper No. 81-0692 April 1981.

4. Beattie, J.R., NASA CR-159688 p.85, Nov. 1979.

5. Rawlin, V.K., Banks, B.A. and Byers, D.C., "Design, Fabrication, and Operation of Dished Accelerator Grids on a 30-cm Ion Thruster", AIAA Paper No. 72-486, April 1972.

6. Collet, C.R., King, H.J. and Schnelker, D.E., "Vectoring of the Beam from Ion Bombardment Thrusters", AIAA Paper No. 71-691, June 1971.

7. Lathem, W.C., "Grid Translation Beam Deflection Systems for 5-cm and 30-cm Diameter Kaufman Thrusters", AIAA Paper No. 72-485, April 1972.

8. Stewart, L.D., Kim, J. and Matsuda, S. "Beam Focusing by Aperture Displacement in Multiampere Ion Sources", Rev. Sci. Instrum. Vol. 46, Sept. 1975, pp. 1193-1196.

9. Homa, J., "Ion Beamlet Vectoring by Grid Translation", appears in "Advanced Space Propulsion Thruster Research", NASA CR-165584, Dec. 1981, pp. 38-60.

10. Davisson, C.J. and Calbick, C.J., Phys. Rev. Vol. 38, 1931, p. 585; Phys. Rev. Vol. 42, 1932, p. 580.

11. Aston, G. and Wilbur, P.J., "Ion Extraction from a Plasma", J. Appl. Phys. Vol. 52, April 1981, pp. 2614-2626.

12. Kaufman, H.R., "Technology of Electron Bombardment Thrusters", appears in "Advances in Electronics and Electron Physics", Academic Press Inc., San Francisco, 1974, p. 330.

13. Rawlin, V.K., Private Communication, Sept. 1982.

14. Rawlin, V.K., Private Communication, June 1982.

15. Aston, G., Kaufman, H.R. and Wilbur, P.J., "Ion Beam Divergence of Two-Grid Accelerator Systems", AIAA Journal, Vol. 16, May 1977, pp. 516-524.

16. Child, C.D., Physical Review, Vol. 32, 1911, pp. 492-511.

17. Aston, G. and Kaufman, H.R., "Ion Beam Divergence Characteristics of Three-Grid Accelerator Systems", AIAA Journal, Vol. 17, Jan. 1979, pp. 64-70.

18. Conrad, J.R., "Beamlet Steering by Aperture Displacement in Ion Sources with Large Acceleration-Deceleration Ratio", Rev. Sci. Instrum. Vol. 51, April 1980, pp. 418-424